Electric Field Reversal of Na_2SO_4, $(NH_4)_2SO_4$, and Na_2CO_3 Relative to $CaCl_2$ and NaCl at the Air/Aqueous Interface Revealed by Heterodyne Detected Phase-Sensitive Sum Frequency

Wei Hua, Aaron M. Jubb, and Heather C. Allen*

Department of Chemistry, The Ohio State University, 100 West 18th Ave, Columbus, Ohio 43210, United States

Ⓢ *Supporting Information*

ABSTRACT: Phase-sensitive sum frequency generation (PS-SFG) spectroscopy, heterodyne detected, was used to investigate the average direction of the transition dipole moment of interfacial water molecules that is intrinsically contained in the sign of the second-order nonlinear susceptibility, $\chi^{(2)}$. The organization of water at air/aqueous inorganic salts interfaces of $CaCl_2$, NaCl, Na_2SO_4, $(NH_4)_2SO_4$, and Na_2CO_3 was inferred. We attribute our findings to the net charge separation arising from the ion distributions at the air/water interface assuming similar ion distribution widths for all systems studied. This is most evident for the aqueous ammonium sulfate solution where the electric field has a greater magnitude relative to the other salt solutions studied. The magnitude of the electric field in the interfacial region decreases in the order $(NH_4)_2SO_4 > Na_2SO_4 > Na_2CO_3 \geq CaCl_2 >$ NaCl; the electric field is opposite in direction for the sulfate and carbonate salts relative to the chloride salts.

SECTION: Surfaces, Interfaces, Catalysis
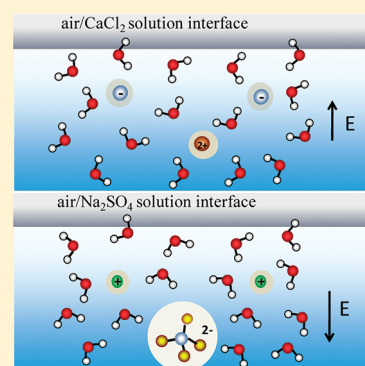
Water organization at the air/aqueous salt solution interface is strongly influenced by ions, specifically, ion distributions that exist in the interfacial region. Revealing the organization of ions and their relative distributions within the air/aqueous interface is critically important for the understanding of processes occurring in every facet of life, from the environment to materials to biology. Interfacial organization of environmentally relevant ions such as those studied in this research has consequences for atmospheric aerosol chemistry,[1,2] thundercloud electrification,[3] geochemistry,[4–8] and ocean surface processes.[9] Particular emphasis in this research is on understanding atmospheric aerosol aging, in which the existence of ions in the aerosol surface and subsurface regions (the interface) plays a critical role for reactivity and accessibility by gas phase oxidants.

To understand the distribution of ions in the interfacial region, we investigate water organization at air/aqueous salt solution interfaces in the presence of $CaCl_2$, NaCl, Na_2SO_4, $(NH_4)_2SO_4$, and Na_2CO_3 using heterodyne-detected phase-sensitive sum frequency generation (PS-SFG). Water organization is directly influenced by the direction and relative strength of the electric field generated in the interfacial region by the distribution of ions. The perturbation of the interfacial water organization by this electric field can involve both reorientation and restructuring of the water hydrogen-bond network as well as an increase in interfacial depth.

PS-SFG is a variant of vibrational sum frequency generation (VSFG). In 1993, the seminal publication of the water surface VSFG spectrum was reported,[10] several years after the first

published accounts of surface VSFG.[11,12] SFG is a second-order nonlinear optical process that provides interface specificity and molecular sensitivity. The SFG response is sensitive to orientation and structuring of interfacial species, although the technique, including PS-SFG, cannot unambiguously separate spectral contributions from water orientation and structure.[2,10,13–18] Moreover, the interface itself is defined by this ordering, and the macroscopic lack on inversion. In the recent past, VSFG has been used extensively to characterize air/aqueous interfaces of acidic, basic, and aqueous salt solutions.[15,16,19,20] Yet the organization of ions at the air/aqueous interface is still not completely understood.

In the past it was accepted that ions were depleted from the aqueous surface, revealing a negative surface excess based on surface tension measurement interpretation.[21–23] This surface depletion is contrary to emerging thought for many ions, specifically halides.[24–28] More recently, however, there is evidence for surface depletion of divalent anions and a proposed reversal of the interfacial electric field for sodium carbonate, as shown in our recent PS-SFG work,[29] for ammonium and sodium sulfate salts, as suggested by previous VSFG studies (conventional) and molecular dynamics simulations,[30] and by a recent PS-SFG study.[31] This is counter for the halide salts from previous studies[24,26,28,32] including recent PS-SFG results as shown by Ji et al. and Tian et al.[27,31,33] Results from PS-SFG studies have
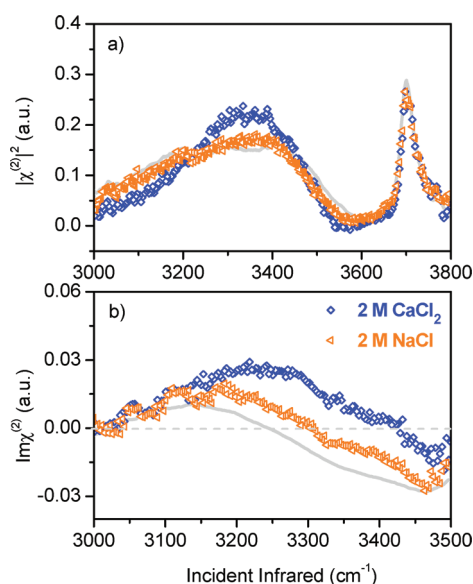
Figure 1. Conventional VSFG $|\chi^{(2)}|^2$ and PS-SFG Im $\chi^{(2)}$ spectra of water molecules at vapor/aqueous solution interfaces of 1.8 M CaCl$_2$ and 1.8 M NaCl salt solutions. (a) $|\chi^{(2)}|^2$ spectra of full 3000–3800 cm^{-1} region (top panel); (b) Im $\chi^{(2)}$ spectra (bottom panel). Neat water spectra are shown as a reference (light gray line). Legend shown in bottom panel corresponds to both panels a and b.

Figure 2. Conventional VSFG $|\chi^{(2)}|^2$ and PS-SFG Im $\chi^{(2)}$ spectra of water molecules at vapor/aqueous solution interfaces of 1.1 M Na$_2$-CO$_3$, 1.1 M Na$_2$SO$_4$, and 1.1 M (NH$_4$)$_2$SO$_4$ salt solutions. (a) $|\chi^{(2)}|^2$ spectra of full 3000–3800 cm^{-1} region (top panel); (b) Im $\chi^{(2)}$ spectra (bottom panel) to 3500 cm^{-1}. Neat water spectra are shown as a reference (light gray line). Legend shown in bottom panel corresponds to both panels a and b.

been critical to the understanding of the interfacial organization of these salt systems although conventional VSFG ($|\chi^{(2)}|^2$) studies have previously inferred this organization indirectly.[24,30]

Conventional VSFG spectroscopy uses homodyne detection; its intensity spectrum is proportional to the absolute square of the second-order nonlinear susceptibility, $|\chi^{(2)}|^2$. Equation 1 shows this proportionality where I_{SFG}, I_{vis}, and I_{IR} are the intensities of the SFG, incident visible, and infrared beams respectively, and $\chi_{NR}^{(2)}$ and $\chi_v^{(2)}$ are the nonresonant and resonant second-order nonlinear susceptibilities, respectively.

$$I_{SFG} \propto |\chi^{(2)}|^2 I_{vis} I_{IR} \propto |\chi_{NR}^{(2)} + \chi_v^{(2)}|^2 I_{vis} I_{IR} \qquad (1)$$

The sign of the complex second-order nonlinear susceptibility, $\chi^{(2)}$, contains transition dipole orientation information, but this information is not directly accessible with conventional VSFG spectroscopic data. PS-SFG spectra reveal the direction of the net interfacial water transition dipole. This is shown from eq 2:

$$\chi_v^{(2)} = \int \frac{A_v \rho(\omega_v)}{\omega_{IR} - \omega_v + i\Gamma_v} \, d\omega_v;$$

$$\text{Im} \, \chi_v^{(2)} = -\int \frac{A_v \Gamma_v \rho(\omega_v)}{(\omega_{IR} - \omega_v)^2 + \Gamma_v^2} \, d\omega_v \qquad (2a, b)$$

where A_v is the transition moment strength, ω_{IR} is the incident infrared frequency, ω_v is the frequency of the vibrational transition, Γ_v is the line width (half width at half-maximum) of the vibrational transition, and $\rho(\omega_v)$ is the density of vibrational modes with frequency of ω_v. PS-SFG is based on interference of the sample SFG response with a phase reference that provides the imaginary part of the nonlinear susceptibility $\chi^{(2)}$, Im $\chi^{(2)}$. Initially, PS-SFG spectroscopy was presented by Shen and co-workers.[27,33–36] Later, Benderskii and co-workers[37] and Tahara and co-workers[38,39] developed this technique for broad bandwidth VSFG systems using heterodyne detection.
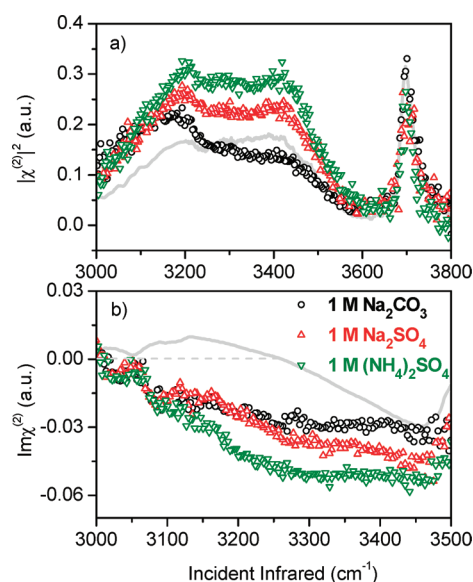
Here we probe the net transition dipole orientation of the interfacial water molecules in the OH stretching region in the presence of calcium and sodium chloride, ammonium and sodium sulfate, and sodium carbonate salts. In the spectra presented here, positive Im $\chi^{(2)}$ refers to SFG active OH transition dipole moments with a net polar orientation directed toward the vapor side of the interface, i.e. hydrogens pointing up. From the PS-SFG data, the relative average distribution of the cations and anions in the interfacial region is then inferred. To this end, both conventional VSFG $|\chi^{(2)}|^2$ spectra and the corresponding PS-SFG Im $\chi^{(2)}$ spectra are presented, followed by further analysis using the Im $\chi^{(2)}$ difference spectra.

Conventional VSFG $|\chi^{(2)}|^2$ and PS-SFG Im $\chi^{(2)}$ spectra of the air/aqueous solution interfaces of CaCl$_2$, NaCl, Na$_2$SO$_4$, (NH$_4$)$_2$SO$_4$, and Na$_2$CO$_3$ salts were obtained and are shown in Figures 1 and 2. The neat water $|\chi^{(2)}|^2$ and Im $\chi^{(2)}$ spectra are shown as a gray line in the same figures for reference. The neat water $|\chi^{(2)}|^2$ spectrum reveals the dangling OH bond of surface water at 3700 cm^{-1} and the broad continuum of hydrogen bond lengths in the lower frequency region from 3000 to 3600 cm^{-1}. In the lowest frequency region shown, it is accepted that these hydrogen bonds are relatively strong, and as one moves to higher frequency, the hydrogen bonding strength is significantly weaker. Additional assignments to this broad continuum continue to be controversial.[35,40–43]

The $|\chi^{(2)}|^2$ spectra of all aqueous salt solutions shown in the first panel of Figures 1 and 2 are consistent with VSFG spectra obtained by others,[2,24,28,30,31,44–46] although the spectrum of CaCl$_2$ has not been previously published. Similar to our work on aqueous MgCl$_2$, the $|\chi^{(2)}|^2$ spectrum in the hydrogen bonding OH stretch region shown by Figure 1a narrows, and the broad continuum OH stretch band is centered close to 3300 cm^{-1}.[47] This is very different relative to aqueous Ca(NO$_3$)$_2$ (and
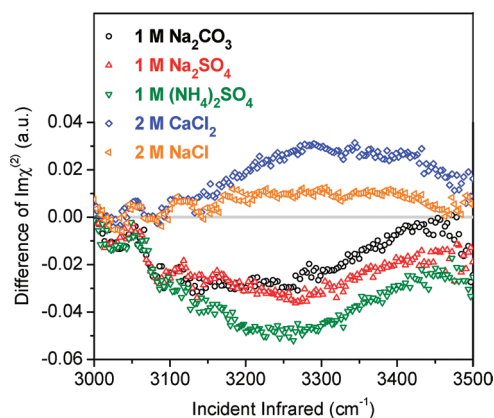
Figure 3. Difference PS-SFG Im $\chi^{(2)}$ spectra (Im $\chi^{(2)}$ salt spectrum minus Im $\chi^{(2)}$ water spectrum) for the indicated salts. These spectra represent qualitative differences between the Im $\chi^{(2)}$ solution spectra and neat water's Im $\chi^{(2)}$ response. Furthermore, here the influence of the respective salt solution on the hydrogen bonding network of water is clear.

Figure 4. Illustration of water orientation at the air/aqueous salt solution interface of (a) 1.8 M $CaCl_2$ and (b) 1.1 M Na_2SO_4 solutions. Calcium and chloride are brown and gray spheres, respectively. Sulfur and oxygen in sulfate ions are blue-gray and yellow spheres, respectively, while sodium ions are green.

$Mg(NO_3)_2$) data that showed a dramatic drop in VSFG signal around 3200 cm^{-1} and large increases around 3400 cm^{-1}.[48] The 3300 cm^{-1} enhancement was interpreted as a weakening of the hydrogen bonding environment in the interfacial region for divalent cation-containing chloride solutions;[47] however, the application of PS-SFG to these systems, e.g., $CaCl_2$ as shown by Figure 1b, necessitates a rethinking of this previous interpretation.

Upon inspection of the Im $\chi^{(2)}$ spectrum of aqueous $CaCl_2$ in Figure 1b, a significant spectral change, larger positive enhancement from 3200 to 3400 cm^{-1} and a less negative intensity for 3400−3500 cm^{-1}, is observed relative to the NaCl and the neat water Im $\chi^{(2)}$ spectra. Only the more weakly hydrogen bonded water molecules have been perturbed by the interfacial electric field. The overall more positive enhancement may be indicative of Ca^{2+} ions being buried further toward the bulk solution so that there is an enhancement of the electric field perpendicular to the surface with Cl$^-$ ions existing above the Ca^{2+} ions. This electric field within the interfacial region reorganizes the interfacial water molecules to have their net OH transition dipole orientation pointing toward the solution surface, along with a probable restructuring of the interfacial water as well as an increasing number of water molecules probed that then increases the interfacial depth. To a lesser extent, in the region around 3475 cm^{-1}, the water molecules are oriented opposite relative to the majority of the hydrogen bonded water molecules. Furthermore, distinguishable after evaluation of the PS-SFG data, the observed decrease at 3200 cm^{-1} and enhancement at 3300 cm^{-1} in the conventional VSFG shown in Figure 1a is the result of spectral convolution of the Im $\chi^{(2)}$ component with the Re $\chi^{(2)}$ component (Supporting Information Figure S1). The Re $\chi^{(2)}$ component of the calcium chloride salt solution features significant differences in intensity and the overall shape changes compared to the Re $\chi^{(2)}$ component of neat water. Therefore, the 3300 cm^{-1} enhancement of the conventional VSFG spectrum is not a decrease in the overall hydrogen bonding environment as was previously suggested for $MgCl_2$.[47] This is a powerful example of the necessity of PS-SFG to study complex systems such as the hydrogen bonding continuum of interfacial water.

The NaCl Im $\chi^{(2)}$ spectrum is slightly more positive for the more weakly hydrogen bonded water molecules compared to neat 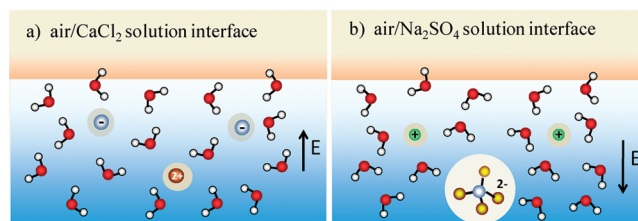water, consistent with the picture that Cl$^-$ has a small surface propensity. The difference Im $\chi^{(2)}$ spectra for the various solutions with respect to the neat water spectrum are plotted in Figure 3, and are solely for ease of assessment and as a qualitative guides for the eyes. The difference spectra reveal that both NaCl and $CaCl_2$ spectra give rise to a greater degree of reorganization featuring more OH transition dipole moments pointing toward the surface of their respective solutions. Clearly, calcium chloride more strongly reorganizes the interfacial water molecules relative to sodium chloride for a similar cation concentration.

Figure 2 shows a comparison between the $|\chi^{(2)}|^2$ and Im $\chi^{(2)}$ spectra from aqueous Na_2CO_3, $(NH_4)_2SO_4$, and Na_2SO_4. As previously observed for conventional VSFG, significant enhancement of the hydrogen bonding region is present and was interpreted, for the most part, as an increase in the field perpendicular to the interface caused by the preference of SO_4^{2-} (and CO_3^{2-}) for increased solvation.[30] Recently both interpretations have been confirmed by PS-SFG data by Tian et al.[31] for both sulfate salts and by Hua et al.[29] for sodium carbonate where all three salts produce a net orientation of the OH transition dipole moments pointing toward the bulk solution. However, after comparison of the three Im $\chi^{(2)}$ spectra, it is clear that $(NH_4)_2SO_4$ reorganizes interfacial water hydrogen bonding to a greater degree, which we attribute to the creation of a significantly larger electric field perpendicular to the interface relative to Na_2CO_3 and Na_2SO_4. The order of largest to smallest electric fields is $(NH_4)_2SO_4$ > Na_2SO_4 > Na_2CO_3, corresponding with the degree of water reorganization. There is a significant difference in the ammonium versus sodium sulfate data, which is clearly observed in the work presented here. The Tian et al.[31] PS-SFG data does not resolve this difference.

As described above, Figure 3 shows a qualitative comparison of the five aqueous salt solutions after subtraction of neat water's Im $\chi^{(2)}$ spectrum from their respective Im $\chi^{(2)}$ spectra. The aqueous $(NH_4)_2SO_4$ causes the greatest disparity relative to neat water (the zero line). Further comparison between salt solution Im $\chi^{(2)}$ spectra reveals the competing preference for hydration of the ions, which culminates in their relative distributions within the interface. Figure 4 illustrates the reversal of the electric field relative to the surface, as is suggested here for chloride and sulfate containing solutions.

Our results can be explained through understanding the hydration properties of each ion. The divalent anions, sulfate and carbonate, exhibit greater propensity for the bulk than the monovalent chloride anions, leading to a larger degree of charge separation between the relative ion distributions. This is consistent with cluster studies showing that divalent anions prefer to reside within the interior of the cluster, while monovalent anions

can exist on the cluster surface.[21,49,50] In addition, the greater PS-SFG Im $\chi^{(2)}$ intensity magnitude observed for $(NH_4)_2SO_4$ solutions versus the Na_2SO_4 is attributed to the surface preference of the ammonium ion.[30] Slight differences in Im $\chi^{(2)}$ signal intensity between Na_2SO_4 and Na_2CO_3 solutions are consistent with the similar charge and hydration radius for these anions. The sulfate ion's slightly smaller hydration radius,[51] and thus greater charge density, may partially explain the slight PS-SFG Im $\chi^{(2)}$ intensity magnitude increase for Na_2SO_4 solutions over Na_2CO_3 solutions, as these factors will influence the respective ion's interfacial distribution. Differences observed for the chloride containing solutions can also be attributed to the surface charge densities of the two cations and thus the larger number of water molecules needed to fully solvate Ca^{2+} versus Na^+ due to the greater valency of calcium. This leads to Ca^{2+} ions on average residing deeper within the interface relative to Na^+.[21,52]

From the PS-SFG data, the Im $\chi^{(2)}$ spectra provide highly informative details: the sign and thus transition dipole orientation of each mode in addition to resonance information. Here we have shown that the sulfate and carbonate anion distributions are well below the surface and that the ammonium and sodium countercation distributions on average preferentially reside closer to the surface. Moreover, ammonium sulfate creates the largest electric field perpendicular to the air/aqueous interface consistent with the picture of ammonium cations having a greater surface propensity relative to sodium cations.

Chloride ions, as discussed by others previously, are accommodated in the surface region, although these anions are less surface active relative to the larger and more polarizable bromide and iodide halides.[21,24,31] Consistent with this, the calcium countercation distributions are shown to exist predominantly below the chloride anion distributions on average. This is opposite to the picture of the counter cations (sodium and ammonium) approaching the surface region for aqueous sulfate and carbonate solutions.

EXPERIMENTAL SECTION

The broad bandwidth VSFG spectrometer and the PS-SFG setup have been described elsewhere,[29,53−55] and more details are provided in the Supporting Information. The polarization combination used for the VSFG and PS-SFG spectra in this study was ssp, where this denotes the polarization for the sum frequency, visible, and infrared beams respectively (s denotes the electric field vector perpendicular to the plane of incidence, and p is parallel to this plane). Only every fourth data point is shown in the SFG spectra to reduce spectral clutter. The phase accuracy with the current optical setup is $20° \pm 5°$ (see Supporting Information for further details in addition to replicate spectra).

For the solution preparation, sodium and ammonium sulfate (ACROS organics $\geq$99% crystalline anhydrous, and Sigma-Aldrich $\geq$99% ACS reagent grade), sodium carbonate (Fisher Scientific, ACS certified 99.5−100.5%), and sodium and calcium chloride (Fisher Scientific ACS certified 99% purity, and USP/FCC 99%) were further purified. (We note that previous studies in our group found that higher purity salts (with higher trace metal purity) proved less pure with respect to organic contamination.) All the salts were heated at 650 °C for 10 h before dissolving in Nanopure water. Nanopure water (not purged of CO_2) with a resistivity of 18.2 to 18.3 M$\Omega\cdot$cm and a measured pH of 5.5 was from a Barnstead Nanopure system (model

D4741) with additional organic removing cartridges (D5026 Type I ORGANICfree Cartridge Kit; Pretreat Feed).

Stock solutions were prepared by dissolving salts in Nanopure water and then filtered using a Whatman Carbon-Cap activate carbon filter usually two to four times to eliminate organic impurities. Raman spectra were used to generate a calibration curve, which then was used for further determining the concentration of each carbonate and sulfate salt. The concentrations of the filtered chloride salt stock solutions were standardized on the basis of the Mohr titration technique,[56] in which silver nitrate (Fisher Scientific, reagent grade) and potassium chromate (E.M. Science, 99.5% purity) were applied as a titrate and an indicator, respectively. The measured concentrations of Na_2SO_4, $(NH_4)_2SO_4$, and Na_2CO_3 were 1.1 M, and their respective pHs were 6.1, 5.4, and 11.7. Concentrations of $CaCl_2$ and NaCl were 1.8 M. All water and salt solutions were proved to be free of organic impurities as revealed by the VSFG spectra obtained in the C−H region of 2800 to 3000 cm^{-1}. All solutions were conditioned at room temperature (23 $\pm$ 1 °C) over 24 h before use.

ASSOCIATED CONTENT

⑤ Supporting Information. The PS-SFG Re $\chi^{(2)}$ spectra of water molecules at vapor/aqueous solution interfaces, experimental methods, and data processing procedures. Replicate PS-SFG spectra illustrating phase accuracy. This material is available free of charge via the Internet at http://pubs.acs.org.

AUTHOR INFORMATION

Corresponding Author
*E-mail: allen@chemistry.ohio-state.edu.

ACKNOWLEDGMENT

REFERENCES

(1) Finlayson-Pitts, B. J.; Pitts, J. N. *Chemistry of the Upper and Lower Troposphere*; Academic Press: San Diego, CA, 2000.

(2) Gopalakrishnan, S.; Liu, D. F.; Allen, H. C.; Kuo, M.; Shultz, M. J. Vibrational Spectroscopic Studies of Aqueous Interfaces: Salts, Acids, Bases, and Nanodrops. *Chem. Rev.* **2006**, *106*, 1155–1175.

(3) Jungwirth, P.; Rosenfeld, D.; Buch, V. A Possible New Molecular Mechanism of Thundercloud Electrification. *Atmos. Res.* **2005**, *76*, 190–205.

(4) Zhang, L.; Tian, C. S.; Waychunas, G. A.; Shen, Y. R. Structures and Charging of α-Alumina (0001)/Water Interfaces Studied by Sum-Frequency Vibrational Spectroscopy. *J. Am. Chem. Soc.* **2008**, *130*, 7686–7694.

(5) Ma, G.; Liu, D.; Allen, H. C. Piperidine Adsorption on Hydrated α-Alumina (0001) Surface Studied by Vibrational Sum Frequency Generation Spectroscopy. *Langmuir* **2004**, *20*, 11620–11629.

(6) Liu, D.; Ma, G.; Allen, H. C. Adsorption of 4-Picoline and Piperidine to the Hydrated SiO_2 Surface: Probing the Surface Acidity with Vibrational Sum Frequency Generation Spectroscopy. *Environ. Sci. Technol.* **2005**, *39*, 2025–2032.

(7) Casillas-Ituarte, N. N.; Allen, H. C. Water, Chloroform, Acetonitrile, and Atrazine Adsorption to the Amorphous Silica Surface Studied by Vibrational Sum Frequency Generation Spectroscopy. *Chem. Phys. Lett.* **2009**, *483*, 84–89.

(8) Xu, M.; Liu, D. F.; Allen, H. C. Ethylenediamine at Air/Liquid and Air/Silica Interfaces: Protonation Versus Hydrogen Bonding Investigated by Sum Frequency Generation Spectroscopy. *Environ. Sci. Technol.* **2006**, *40*, 1566–1572.

(9) Lass, K.; Kleber, J.; Friedrichs, G. Vibrational Sum-Frequency Generation as a Probe for Composition, Chemical Reactivity, and Film Formation Dynamics of the Sea Surface Nanolayer. *Limnol. Oceanogr.: Methods* **2010**, *8*, 216–228.

(10) Du, Q.; Superfine, R.; Freysz, E.; Shen, Y. R. Vibrational Spectroscopy of Water at the Vapor Water Interface. *Phys. Rev. Lett.* **1993**, *70*, 2313–2316.

(11) Superfine, R.; Huang, J. Y.; Shen, Y. R. Nonlinear Optical Studies of the Pure Liquid/Vapor Interface: Vibrational Spectra and Polar Ordering. *Phys. Rev. Lett.* **1991**, *66*, 1066–1069.

(12) Zhu, X. D.; Suhr, H.; Shen, Y. R. Surface Vibrational Spectroscopy by Infrared-Visible Sum Frequency Generation. *Phys. Rev. B: Condens. Matter Mater. Phys.* **1987**, *35*, 3047–3050.

(13) Du, Q.; Freysz, E.; Shen, Y. R. Surface Vibrational Spectroscopic Studies of Hydrogen Bonding and Hydrophobicity. *Science* **1994**, *264*, 826–828.

(14) Shultz, M. J.; Schnitzer, C.; Simonelli, D.; Baldelli, S. Sum Frequency Generation Spectroscopy of the Aqueous Interface. Ionic and Soluble Molecular Solutions. *Int. Rev. Phys. Chem.* **2000**, *19*, 123–153.

(15) Richmond, G. L. Molecular Bonding and Interactions at Aqueous Surfaces as Probed by Vibrational Sum Frequency Spectroscopy. *Chem. Rev.* **2002**, *102*, 2693–2724.

(16) Shen, Y. R.; Ostroverkhov, V. Sum-Frequency Vibrational Spectroscopy on Water Interfaces: Polar Orientation of Water Molecules at Interfaces. *Chem. Rev.* **2006**, *106*, 1140–1154.

(17) Fan, Y. B.; Chen, X.; Yang, L. J.; Cremer, P. S.; Gao, Y. Q. On the Structure of Water at the Aqueous/Air Interface. *J. Phys. Chem. B* **2009**, *113*, 11672–11679.

(18) Wang, H. F.; Gan, W.; Lu, R.; Rao, Y.; Wu, B. H. Quantitative Spectral and Orientational Analysis in Surface Sum Frequency Generation Vibrational Spectroscopy (SFG-VS). *Int. Rev. Phys. Chem.* **2005**, *24*, 191–256.

(19) Shultz, M. J.; Baldelli, S.; Schnitzer, C.; Simonelle, D. Aqueous Solution/Air Interfaces Probed with Sum Frequency Generation Spectroscopy. *J. Phys. Chem. B* **2002**, *106*, 5313–5324.

(20) Allen, H. C.; Casillas-Ituarte, N. N.; Sierra-Hernandez, M. R.; Chen, X. K.; Tang, C. Y. Shedding Light on Water Structure at Air–Aqueous Interfaces: Ions, Lipids, and Hydration. *Phys. Chem. Chem. Phys.* **2009**, *11*, 5538–5549.

(21) Jungwirth, P.; Tobias, D. J. Specific Ion Effects at the Air/Water Interface. *Chem. Rev.* **2006**, *106*, 1259–1281.

(22) Tobias, D. J.; Hemminger, J. C. Chemistry - Getting Specific About Specific Ion Effects. *Science* **2008**, *319*, 1197–1198.

(23) Gibbs, J. W. *The Collected Works of J. Willard. Gibbs*; Longmans: New York, 1928.

(24) Liu, D. F.; Ma, G.; Levering, L. M.; Allen, H. C. Vibrational Spectroscopy of Aqueous Sodium Halide Solutions and Air–Liquid Interfaces: Observation of Increased Interfacial Depth. *J. Phys. Chem. B* **2004**, *108*, 2252–2260.

(25) Mucha, M.; Frigato, T.; Levering, L. M.; Allen, H. C.; Tobias, D. J.; Dang, L. X.; Jungwirth, P. Unified Molecular Picture of the Surfaces of Aqueous Acid, Base, and Salt Solutions. *J. Phys. Chem. B* **2005**, *109*, 7617–7623.

(26) Petersen, P. B.; Saykally, R. J. Evidence for an Enhanced Hydronium Concentration at the Liquid Water Surface. *J. Phys. Chem. B* **2005**, *109*, 7976–7980.

(27) Ji, N.; Ostroverkhov, V.; Tian, C. S.; Shen, Y. R. Characterization of Vibrational Resonances of Water–Vapor Interfaces by Phase-Sensitive Sum-Frequency Spectroscopy. *Phys. Rev. Lett.* **2008**, *100*, 096102–096104.

(28) Raymond, E. A.; Richmond, G. L. Probing the Molecular Structure and Bonding of the Surface of Aqueous Salt Solutions. *J. Phys. Chem. B* **2004**, *108*, 5051–5059.

(29) Hua, W.; Chen, X. K.; Allen, H. C. Phase-Sensitive Sum Frequency Revealing Accommodation of Bicarbonate Ions, and Charge Separation of Sodium and Carbonate Ions within the Air/Water Interface. *J. Phys. Chem. A* **2011**, *115*, 6233–6238.

(30) Gopalakrishnan, S.; Jungwirth, P.; Tobias, D. J.; Allen, H. C. Air—Liquid Interfaces of Aqueous Solution Containing Ammonium and Sulfate: Spectroscopic and Molecular Dynamics Studies. *J. Phys. Chem. B* **2005**, *109*, 8861–8872.

(31) Tian, C. S.; Byrnes, S. J.; Han, H. L.; Shen, Y. R. Surface Propensities of Atmospherically Relevant Ions in Salt Solutions Revealed by Phase-Sensitive Sum Frequency Vibrational Spectroscopy. *J. Phy. Chem. Lett.* **2011**, *2*, 1946–1949.

(32) Ghosal, S.; Hemminger, J. C.; Bluhm, H.; Mun, B. S.; Hebenstreit, E. L. D.; Ketteler, G.; Ogletree, D. F.; Requejo, F. G.; Salmeron, M. Electron Spectroscopy of Aqueous Solution Interfaces Reveals Surface Enhancement of Halides. *Science* **2005**, *307*, 563–566.

(33) Tian, C. S.; Ji, N.; Waychunas, G. A.; Shen, Y. R. Interfacial Structures of Acidic and Basic Aqueous Solutions. *J. Am. Chem. Soc.* **2008**, *130*, 13033–13039.

(34) Tian, C. S.; Shen, Y. R. Isotopic Dilution Study of the Water/Vapor Interface by Phase-Sensitive Sum-Frequency Vibrational Spectroscopy. *J. Am. Chem. Soc.* **2009**, *131*, 2790–2791.

(35) Tian, C. S.; Shen, Y. R. Sum-Frequency Vibrational Spectroscopic Studies of Water/Vapor Interfaces. *Chem. Phys. Lett.* **2009**, *470*, 1–6.

(36) Tian, C. S.; Shen, Y. R. Structure and Charging of Hydrophobic Material/Water Interfaces Studied by Phase-Sensitive Sum-Frequency Vibrational Spectroscopy. *Proc. Natl. Acad. Sci. U.S.A.* **2009**, *106*, 15148–15153.

(37) Stiopkin, I. V.; Jayathilake, H. D.; Bordenyuk, A. N.; Benderskii, A. V. Heterodyne-Detected Vibrational Sum Frequency Generation Spectroscopy. *J. Am. Chem. Soc.* **2008**, *130*, 2271–2275.

(38) Nihonyanagi, S.; Yamaguchi, S.; Tahara, T. Direct Evidence for Orientational Flip-Flop of Water Molecules at Charged Interfaces: A Heterodyne-Detected Vibrational Sum Frequency Generation Study. *J. Chem. Phys.* **2009**, *130*, 204704–204708.

(39) Nihonyanagi, S.; Yamaguchi, S.; Tahara, T. Water Hydrogen Bond Structure near Highly Charged Interfaces Is Not Like Ice. *J. Am. Chem. Soc.* **2010**, *132*, 6867–6869.

(40) Sovago, M.; Campen, R. K.; Bakker, H. J.; Bonn, M. Hydrogen Bonding Strength of Interfacial Water Determined with Surface Sum-Frequency Generation. *Chem. Phys. Lett.* **2009**, *470*, 7–12.

(41) Raymond, E. A.; Tarbuck, T. L.; Brown, M. G.; Richmond, G. L. Hydrogen-Bonding Interactions at the Vapor/Water Interface Investigated by Vibrational Sum-Frequency Spectroscopy of HOD/H_2O/D_2O Mixtures and Molecular Dynamics Simulations. *J. Phys. Chem. B* **2003**, *107*, 546–556.

(42) Ishiyama, T.; Morita, A. Analysis of Anisotropic Local Field in Sum Frequency Generation Spectroscopy with the Charge Response Kernel Water Model. *J. Chem. Phys.* **2009**, *131*, 244714–244717.

(43) Auer, B. M.; Skinner, J. L. Vibrational Sum-Frequency Spectroscopy of the Water Liquid/Vapor Interface. *J. Phys. Chem. B* **2009**, *113*, 4125–4130.

(44) Tarbuck, T. L.; Richmond, G. L. Adsorption and Reaction of CO_2 and SO_2 at a Water Surface. *J. Am. Chem. Soc.* **2006**, *128*, 3256–3267.

(45) Du, H.; Liu, J.; Ozdemir, O.; Nguyen, A. V.; Miller, J. D. Molecular Features of the Air/Carbonate Solution Interface. *J. Colloid Interface Sci.* **2008**, *318*, 271–277.

(46) Ishiyama, T.; Morita, A. Molecular Dynamics Study of Gas-Liquid Aqueous Sodium Halide Interfaces. II. Analysis of Vibrational Sum Frequency Generation Spectra. *J. Phys. Chem. C* **2007**, *111*, 738–748.

(47) Casillas-Ituarte, N. N.; Callahan, K. M.; Tang, C. Y.; Chen, X. K.; Roeselova, M.; Tobias, D. J.; Allen, H. C. Surface Organization of Aqueous $MgCl_2$ and Application to Atmospheric Marine Aerosol Chemistry. *Proc. Natl. Acad. Sci. U.S.A.* **2010**, *107*, 6616–6621.

(48) Xu, M.; Spinney, R.; Allen, H. C. Water Structure at the Air—Aqueous Interface of Divalent Cation and Nitrate Solutions. *J. Phys. Chem. B* **2009**, *113*, 4102–4110.

(49) Jungwirth, P.; Curtis, J. E.; Tobias, D. J. Polarizability and Aqueous Solvation of the Sulfate Dianion. *Chem. Phys. Lett.* **2003**, *367*, 704–710.

(50) Wang, X. B.; Yang, X.; Nicholas, J. B.; Wang, L. S. Bulk-like Features in the Photoemission Spectra of Hydrated Doubly Charged Anion Clusters. *Science* **2001**, *294*, 1322–1325.

(51) dos Santos, A. P.; Diehl, A.; Levin, Y. Surface Tensions, Surface Potentials, and the Hofmeister Series of Electrolyte Solutions. *Langmuir* **2010**, *26*, 10778–10783.

(52) Bush, M. F.; Saykally, R. J.; Williams, E. R. Infrared Action Spectra of $Ca^{2+}(H_2O)(11-69)$ Exhibit Spectral Signatures for Condensed-Phase Structures with Increasing Cluster Size. *J. Am. Chem. Soc.* **2008**, *130*, 15482–15489.

(53) Tang, C. Y.; Allen, H. C. Ionic Binding of Na^+ versus K^+ to the Carboxylic Acid Headgroup of Palmitic Acid Monolayers Studied by Vibrational Sum Frequency Generation Spectroscopy. *J. Phys. Chem. A* **2009**, *113*, 7383–7393.

(54) Chen, X. K.; Hua, W.; Huang, Z. S.; Allen, H. C. Interfacial Water Structure Associated with Phospholipid Membranes Studied by Phase-Sensitive Vibrational Sum Frequency Generation Spectroscopy. *J. Am. Chem. Soc.* **2010**, *132*, 11336–11342.

(55) Chen, X. K.; Allen, H. C. Water Structure at Aqueous Solution Surfaces of Atmospherically Relevant Dimethyl Sulfoxide and Methanesulfonic Acid Revealed by Phase-Sensitive Sum Frequency Spectroscopy. *J. Phys. Chem. B* **2010**, *114*, 14983–14988.

(56) Finlayson, A. C. The pH Range of the Mohr Titration for Chloride-Ion Can Be Usefully Extended to 4—10.5. *J. Chem. Educ.* **1992**, *69*, 559–559.